nature synthesis

Article

https://doi.org/10.1038/s44160-024-00661-y

Mechanochemical nitrogen fixation catalysed by molybdenum complexes

Received: 24 April 2024

Accepted: 6 September 2024

Shun Suginome[1], **Kurumi Murota**[1], **Akira Yamamoto**[2], **Hisao Yoshida**[2] & **Yoshiaki Nishibayashi**[1] ✉

Transition metal-catalysed mechanochemical reactions using ball milling have emerged as important tools to realize unique organic transformations. Mechanochemical reactions have advantages over conventional homogeneous reactions, such as using a small amount of organic solvent, having a broad substrate scope and being generally fast and selective reactions. An increasing number of mechanochemical reactions between solid substrates have been examined, but only a few examples of mechanochemical reactions involving gaseous substrates, such as nitrogen fixation to convert dinitrogen into ammonia, have been reported until now. Here we develop catalytic mechanochemical nitrogen fixation using molybdenum complexes as molecular catalysts. An atmospheric pressure of dinitrogen was reacted with samarium diiodide as a reductant and water or alcohols as proton sources in the presence of the molybdenum catalysts, using ball milling under solvent-free and near-ambient reaction conditions to afford up to 860 equivalents of ammonia based on the catalyst. In addition, we demonstrated that even insoluble cellulose can be applied as the proton source. Further, we revealed that the molybdenum-catalysed mechanochemical nitrogen fixation proceeds via nitrogen–nitrogen bond cleavage at the gas–solid interface and nitrogen–hydrogen bond formation in the solid phase.

Recently, mechanochemical reactions using the ball-milling technique have emerged as novel tools for organic transformations catalysed by transition metal complexes[1–5]. Contrary to conventional organic reactions under homogeneous conditions, where all the reactants are dissolved in solvents, mechanochemical reactions proceed without or with a small amount of organic solvent[6–21]. This unique feature of mechanochemical reactions—organic transformation in the solid phase—can not only reduce the required amount of toxic organic solvents but also expand the substrate scope of transition metal-catalysed reactions into insoluble compounds[7,10–12]. In addition, the catalytic reactions of organic compounds proceed in higher yields[18,19] or with a higher selectivity[8,9,17] under mechanochemical conditions than under homogeneous conditions.

In contrast to the increasing reports of mechanochemical reactions between solid substrates[6–19], several mechanochemical reactions involving gaseous reactants catalysed by transition metal complexes have been reported (Fig. 1a)[20–22]. However, the direct use of (not in situ formed) gaseous reactants in mechanochemical reactions catalysed by transition metal complexes is still scarce. Considering a number of transition metal-catalysed molecular transformations using gaseous reactants in industry and in chemistry textbooks (for example, the Wacker process[23], olefin polymerization[24,25] and asymmetric hydrogenation[26]), there is plenty of room for the exploration of reactivities unique to the mechanochemical reactions at the interface of the gas phase and the solid phase.

Among molecular transformations using gaseous reactants, nitrogen fixation, the process of converting earth-abundant but unreactive dinitrogen (N_2) into ammonia (NH_3), is one of the most essential and challenging processes[27–29]. Nowadays, NH_3 is becoming more and more important not only as a useful feedstock but as a clean energy carrier

---

[1]Department of Applied Chemistry, School of Engineering, The University of Tokyo, Tokyo, Japan. [2]Graduate School of Human and Environmental Studies, Kyoto University, Kyoto, Japan. ✉e-mail: ynishiba@g.ecc.u-tokyo.ac.jp

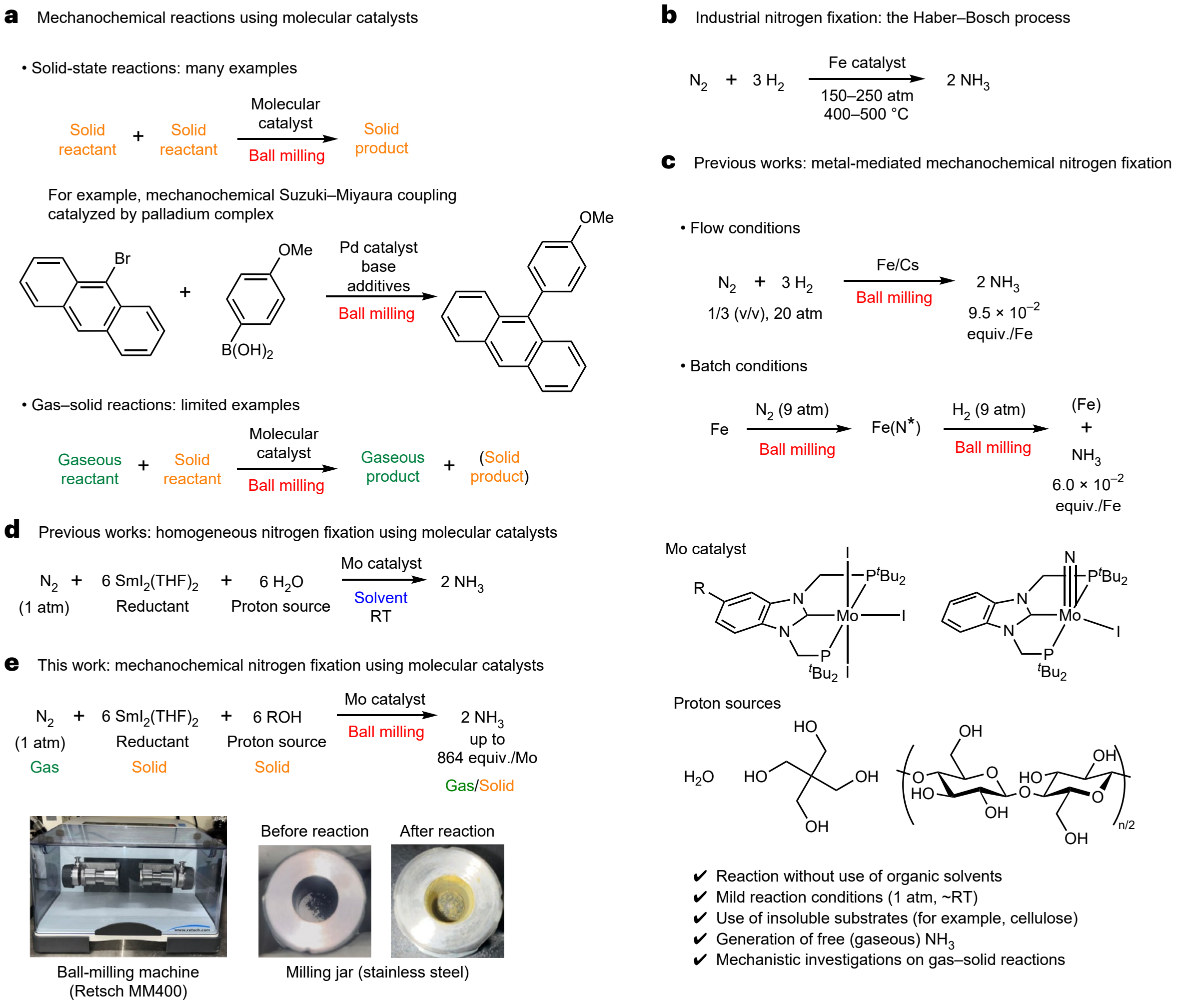

Fig. 1 | Mechanochemical reactions of gaseous reactants using molecular catalysts. a, Mechanochemical reactions using molecular catalysts between two or more solid reactants (well explored)[6–19] or those involving gaseous reactants (unexplored)[20–22]. **b**, The Haber–Bosch process. **c**, Previous works: mechanochemical nitrogen fixation mediated by iron metal[30,31]. **d**, Previous works: homogeneous nitrogen fixation using molybdenum catalysts[36,37]. **e**, This work: mechanochemical nitrogen fixation using molybdenum catalysts. RT, room temperature.

that does not emit carbon dioxide (CO_2) during its combustion. In industry, NH_3 is produced by the Haber–Bosch process from N_2 and dihydrogen (H_2) catalysed by heterogeneous iron-based catalysts under very harsh reaction conditions (Fig. 1b). The process is accompanied by a massive energy consumption and a considerable amount of CO_2 emission for the preparation of H_2 and for the high-temperature and high-pressure conditions. Therefore, there is a growing demand for the development of an environmentally friendly nitrogen fixation process. Quite recently, several groups reported NH_3 formation under mechanochemical conditions by the reaction of N_2 with H_2 mediated by iron or titanium metals (Fig. 1c)[30–32]. By adopting mechanochemical conditions, the reactions proceeded under relatively mild reaction conditions (pressure less than 20 atm and temperature close to room temperature). However, unfortunately, the total amounts of produced NH_3 were less than the stoichiometric amount based on the metals, that is, the reactions are not catalytic.

Our group and others have contributed to the development of catalytic nitrogen fixation from different aspects to the Haber–Bosch process by using transition metal complexes as catalysts under homogeneous conditions[33–42]. Employing a homogeneous reaction system catalysed by transition metal complexes, N_2 can be converted to NH_3 by reactions with reductants and proton sources at atmospheric pressure and room temperature or lower. We have achieved nitrogen fixation employing samarium diiodide (SmI_2) as a reductant and water as a proton source with molybdenum complexes bearing pincer-type ligands as catalysts in tetrahydrofuran (THF) under ambient reaction conditions (Fig. 1d)[36,37]. The catalysts have already reached a high turnover number (up to 60,000) towards NH_3 formation in the homogeneous reaction system. However, the use of large amounts of organic solvents, which are expensive and not eco-friendly, will be one of the obstacles to the practical application.

Here, we have developed the catalytic mechanochemical nitrogen fixation using $SmI_2(THF)_2$ as a reductant and water or alcohols as proton sources in the presence of the catalytic amount of molybdenum complexes under solvent-free and mild (at atmospheric pressure and near room temperature) reaction conditions (Fig. 1e). This was achieved by redesigning our homogeneous reactions in solution for mechanochemical reactions at the gas–solid interface. Notably, specific alcohols, such as cellulose, served as much better proton sources under mechanochemical conditions than under homogeneous conditions. Finally, we revealed that the mechanochemical nitrogen fixation proceeds through nitrogen–nitrogen bond cleavage at the molecular catalysts and nitrogen–hydrogen bond formation by proton-coupled electron transfer (PCET) processes, both of which are unprecedented in mechanochemical reactions. We believe that the results presented in this work pave the way for the discovery of novel reactivity in mechanochemical reactions.

Results and discussion

Development of mechanochemical nitrogen fixation

We first examined the mechanochemical reactions presented in Table 1 based on the reactions under homogeneous conditions[36,37]. All reactions were conducted in a Retsch MM400 shaker mill with a 5 ml stainless-steel milling jar and a 10 mm stainless-steel ball without external heating. An atmospheric pressure of N_2 reacted with 180 equiv. of samarium diiodide THF adduct ($SmI_2(THF)_2$) and 180 equiv. of water in the presence of a molybdenum triiodide complex bearing a phosphine–carbene–phosphine (PCP)-type pincer ligand (**1a**) by ball milling at 30 Hz for 1 h to give 30 equiv. of NH_3 (based on **1a**) together with 14 equiv. of H_2 (based on **1a**) as a by-product (Table 1, entry 1). Note that neither hydrazine nor gaseous by-product other than H_2 was detected in any entries (Supplementary Fig. 17). After the reaction, the dark-blue colour of the starting material turned yellow (characteristic of Sm(III) species), which clearly indicates the consumption of $SmI_2(THF)_2$ during the mechanochemical reaction (Supplementary Figs. 3a,b). When reactions were conducted in the absence of N_2, SmI_2, H_2O or **1a**, almost no NH_3 was formed in all cases (Table 1, entries 2–5), suggesting that the reaction proceeds following the equation in Table 1. Ball milling is essential for the mechanochemical nitrogen fixation, since almost no NH_3 was formed when the reaction was carried out with magnetic stirring in a flask in the absence of solvent (Table 1, entry 6). The addition of a small amount of organic solvent ('liquid-assisted grinding' method[43]) effective for some mechanochemical reactions did not improve the catalytic activity towards NH_3, but rather increased the amount of H_2 (Supplementary Table 1, entry 2).

Then, we investigated the scope of proton sources in the mechanochemical nitrogen fixation. In contrast to the reactions using water as a proton source, the use of alcoholic proton sources employed in homogeneous reactions[36], such as methanol (MeOH), ethanol (EtOH) and ethylene glycol, resulted in lower catalytic activities towards NH_3 formation (Table 1, entries 7–9). We wondered whether one of the reasons for such low catalytic activities is the immediate formation of H_2 by the direct reaction between $SmI_2(THF)_2$ and liquid proton sources during (or even before) ball-milling processes. To solve this issue, we next carried out the mechanochemical nitrogen fixation using solid proton sources. After a thorough investigation of solid proton sources (Supplementary Table 2, entries 7–16), we found that the use of a tetravalent solid alcohol, pentaerythritol, substantially improved the amount of NH_3 to 49 equiv. based on the catalyst (Table 1, entry 10). We also examined reactions using pentaerythritol (0.18 mmol, tetravalent alcohol), neopentyl glycol (0.36 mmol, divalent alcohol) and neopentyl alcohol (0.72 mmol, monovalent alcohol) as solid proton sources to give 46, 31 and 18 equiv. of NH_3 based on the catalyst **1a**, respectively (Supplementary Table 3). The results suggest that not only the phase of proton sources (solid or liquid) but also the multivalency of the alcohol are important factors for higher catalytic activities. Encouraged by this observation, we turned our attention to sugars as solid and multivalent alcohols. When D-glucose was used as a proton source, NH_3 was formed in a good yield without the formation of H_2 (Table 1, entry 11). Quite interestingly, cellulose, which is an abundant biopolymer but insoluble in almost all organic solvents[44], can also be employed as a proton source to give NH_3 in a high yield with an excellent selectivity (Table 1, entry 12). This is in sharp contrast to the homogeneous reaction in THF using cellulose as a proton source, where almost no NH_3 was produced (Table 1, entry 13).

We investigated the time profiles of reactions using cellulose as a proton source, under either mechanochemical conditions by ball milling or homogeneous conditions in THF. As shown in Fig. 2a, mechanochemical reaction (Fig. 2a, red) completed within 2 h and was much faster than the homogeneous reaction using THF, where almost no NH_3 formation was observed probably due to the low solubility of cellulose (Fig. 2a, blue). These results clearly demonstrate the advantage of mechanochemical nitrogen fixation towards insoluble substrates.

Table 1 | Mechanochemical nitrogen fixation using various proton sources

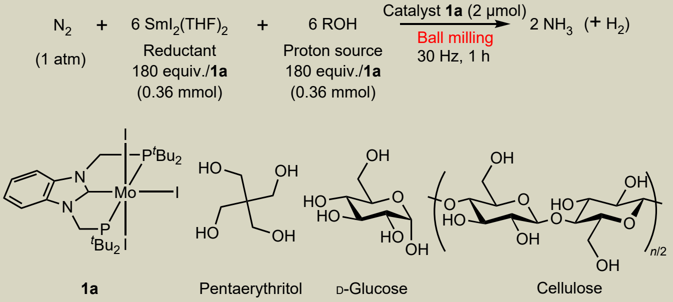

Entry	Proton sources	NH_3 (equiv./1a)	NH_3 (%)	H_2 (equiv./1a)	H_2 (%)
1[a]	H_2O	29.5±0.5	48	13.9±3.7	15
2[b]	H_2O	–	0	–	30
3[c]	H_2O	0	0	26.8	28
4[d]	H_2O	0	0	2.9	3
5	–	1.5	2	0.3	0.3
6[e]	H_2O	1.0	2	12.3	13
7[a]	MeOH	10.3±1.3	18	16.4±1.8	19
8[a]	EtOH	21.9±2.6	38	20.0±1.6	23
9	Ethylene glycol	11.6	19	28.2	31
10[a]	Pentaerythritol	48.9±0.9	81	14.3±6.6	16
11[a]	D-Glucose	33.1±3.6	56	1.8±0.2	2
12[a,f]	Cellulose	43.5±1.7	74	0.6±0.3	0.9
13[f,g]	Cellulose	3.0	5	0	0

[a] Data are the mean of multiple individual experiments (at least two) with error bars representing standard deviation. [b] Reaction without catalyst **1a**. [c] Reaction under Ar for 15 min. [d] Reaction without $SmI_2(THF)_2$. [e] Reaction with magnetic stirring. [f] Reaction for 2 h. [g] Reaction in THF.

One thing to note is an induction period (of around 30 min) observed in the mechanochemical reaction using cellulose as a proton source (Fig. 2a, red) in contrast to those using pentaerythritol (Supplementary Fig. 4). We consider that this is due to the relatively slow formation of some active species towards NH_3 formation between $SmI_2(THF)_2$ and cellulose analogous to the formation of $SmI_2(H_2O)$ complex (vide infra) as an active species under homogeneous conditions[45]. To verify this hypothesis, $SmI_2(THF)_2$ and cellulose were reacted by ball milling at 30 Hz for 2 h under Ar atmosphere before the catalytic reaction. In this case, 24 equiv. of NH_3 were formed by the mechanochemical reaction for 30 min in contrast to the reaction for 30 min under standard conditions to afford only 6 equiv. of NH_3 based on the catalyst. We also examined the mechanochemical reaction for 30 min using cellulose pre-treated by ball milling at 30 Hz for 2 h; however, only 3 equiv. of NH_3 were formed. Therefore, we suppose that the formation of active species between $SmI_2(THF)_2$ and proton sources plays an important role during mechanochemical nitrogen fixation.

In addition, we measured diffuse-reflectance ultraviolet–visible (UV–vis) spectra of the mixture of $SmI_2(THF)_2$ and proton sources after ball milling to analyse the active species formed during the reaction (Fig. 2b and Supplementary Fig. 16). The UV–vis spectrum of the mixture of $SmI_2(THF)_2$ and 10 equiv. of cellulose ball milled for 2 h under an atmospheric pressure of Ar (Fig. 2b, solid purple line) showed disappearance of absorption band around 700 nm from that of $SmI_2(THF)_2$ (Fig. 2b, solid blue line). We also observed that $SmI_2(THF)_2$ underwent similar colour change after ball milling with 10 equiv. of pentaerythritol for 10 min under an atmospheric pressure of Ar (Supplementary

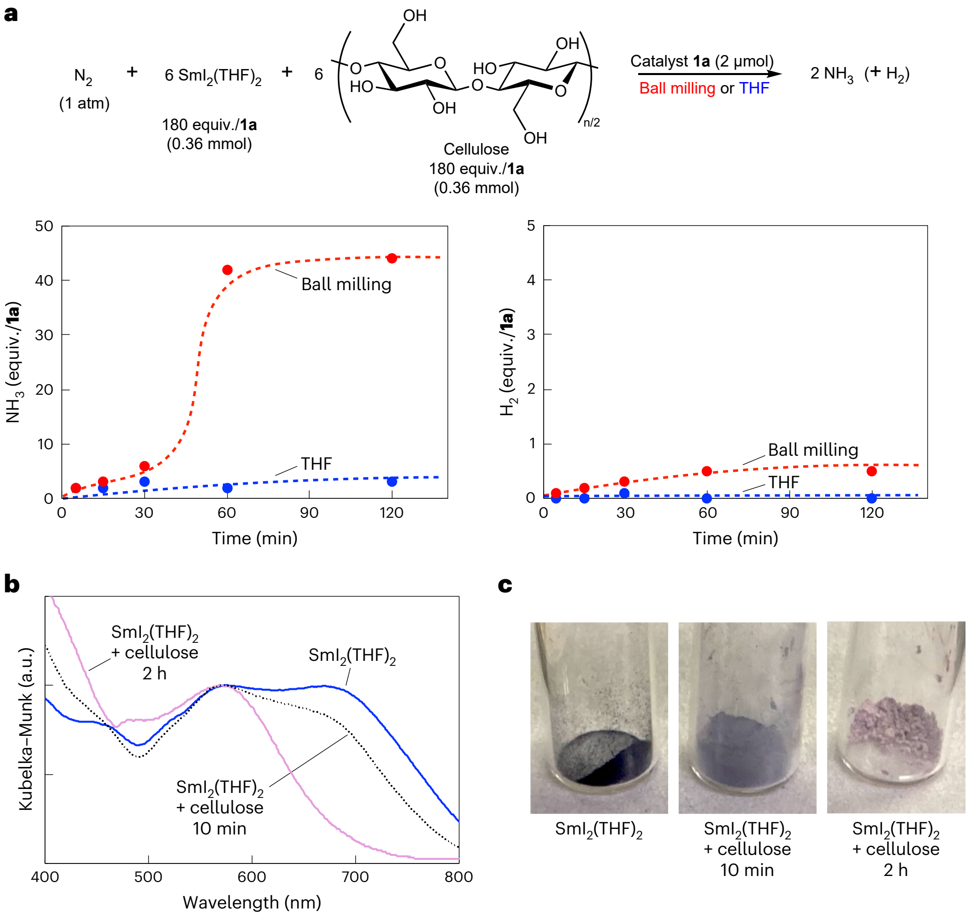

Fig. 2 | Time courses of NH_3 and H_2 formation in the mechanochemical nitrogen fixation and characterization of reactive intermediates. a, The time courses of NH_3 (bottom left) and H_2 formation (bottom right) when an atmospheric pressure of dinitrogen was reacted (top) with $SmI_2(THF)_2$ (0.36 mmol) and cellulose (0.36 mmol based on a repeating unit) in the presence of **1a** (2 µmol) under either mechanochemical (by ball milling, red) or homogeneous (in THF, blue) conditions. The data points indicate the amount of formed NH_3 or H_2 after the reaction for 5, 15, 30, 60 or 120 min, and the dashed curves represent the presence or absence of the induction period. **b**, UV–vis diffuse-reflectance spectra of $SmI_2(THF)_2$ (blue), the mixture of $SmI_2(THF)_2$ (0.12 mmol) and cellulose (1.2 mmol) ball milled for 10 min (black dotted) or 2 h (purple). **c**, Photos of $SmI_2(THF)_2$ and the mixture of $SmI_2(THF)_2$ (0.12 mmol) and cellulose (1.2 mmol) ball milled for 10 min or 2 h.

Fig. 16b). These observed colour change in both cases was similar to the colour change of the reaction mixture by the addition of a large excess of water (150 equiv.) to a THF solution of $SmI_2(THF)_2$ to afford a water-coordinated Sm complex such as $[Sm(H_2O)_8]I_2$(ref. 45). Thus, the diffuse-reflectance UV–vis studies suggest that cellulose coordinates to $SmI_2(THF)_2$ after ball milling for a certain period and served as an active species. On the other hand, only a slight change in the UV–vis spectra was observed when $SmI_2(THF)_2$ and 10 equiv. of cellulose were ball milled for 10 min under an atmospheric pressure of Ar, indicating that the active species was not formed (Fig. 2b, dotted black line). This slow formation of the active species corresponds well with the observed induction period in the time profile of NH_3 formation in Fig. 2a. Further, we obtained a dinuclear Sm(III)–pentaerythritol complex as colourless crystals by the mechanochemical reaction between $SmI_2(THF)_2$ and 10 equiv. of pentaerythritol for 10 min and subsequent recrystallization from $MeOH/Et_2O$, although we isolated only a small amount of this complex in pure form (Supplementary Fig. 18). X-ray analysis reveals that the Sm centre was oxidized from Sm(II) to Sm(III) together with the loss of 1 equiv. of protons of coordinated pentaerythritol. The obtained structure may support the formation of the complex between $SmI_2(THF)_2$ and proton sources as active species under mechanochemical conditions.

We examined other molybdenum catalysts for mechanochemical nitrogen fixation by employing pentaerythritol as a proton source (Table 2). Molybdenum complex bearing a phosphine–pyridine–phosphine (PNP)-type pincer ligand (**3**) also served as a catalyst but resulted in only a lower yield (18 equiv./Mo; Table 2, entry 7). We then examined molybdenum(0) complexes bearing simple phosphine ligands. Interestingly, *trans*-$[Mo(N_2)_2(PPh_2Me)_4]$ (**4**) showed catalytic activity towards NH_3 formation under mechanochemical conditions (8 equiv./Mo; Table 2, entry 8), while *trans*-$[Mo(N_2)_2(dppe)_2]$ (**5**, dppe, 1,2-bis-(diphenylphosphino)ethane)) did not show any catalytic activity (Table 2, entry 9)[46]. We separately confirmed that the reaction in the presence of a catalytic amount of molybdenum(0) or molybdenum oxide (MoO_3) powder did not generate any NH_3 (Table 2, entries 10 and 11); therefore, we could rule out the possibility that the inorganic compounds generated by degradation of the molybdenum complexes during the ball-milling process worked as catalysts. Finally, we found that a molybdenum complex bearing a PCP-type pincer ligand with trifluoromethyl group (**1b**) exhibits one of the best results in the present reaction conditions (49 equiv./Mo; Table 2, entry 4). Then, we optimized the reaction conditions by reducing the amount of the catalysts **1a** or **1b**. When an atmospheric pressure of N_2 was reacted with 3,600 equiv. of $SmI_2(THF)_2$ and 3,600 equiv. of pentaerythritol in the presence of the catalyst **1a** and **1b** (0.1 µmol) for 1 h under mechanochemical conditions, 450 equiv. and 860 equiv. of NH_3 based on the catalysts were produced, respectively (Table 2, entries 3 and 5).

Table 2 | Mechanochemical nitrogen fixation using various molybdenum catalysts

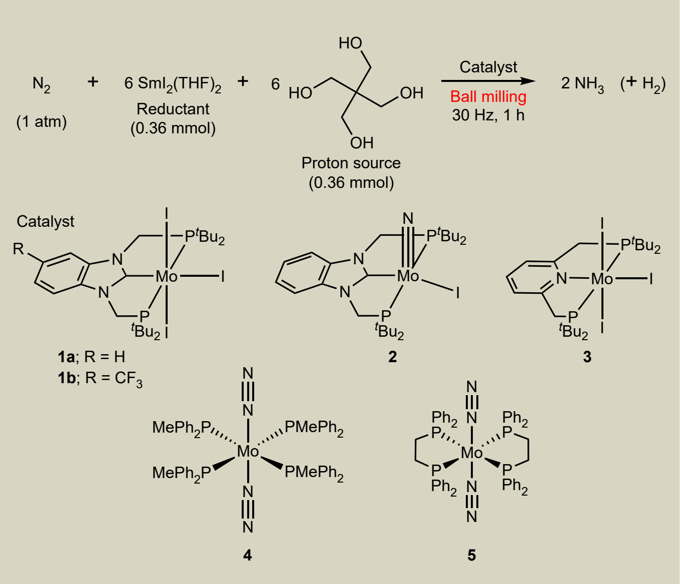

Entry	cat.	Amount of catalyst (μmol)	NH_3 (equiv./Mo)	NH_3 (%)	H_2 (equiv./Mo)	H_2 (%)
1[a,b]	**1a**	2	48.9±0.9	81	14.3±6.6	16
2	**1a**	0.25	362	75	45.1	6
3[a]	**1a**	0.1	449±102	37	160±17	9
4	**1b**	2	48.8	83	7.0	8
5[a]	**1b**	0.1	864±30	72	76.2±19.2	4
6	**2**	2	43.7	82	7.1	9
7	**3**	2	17.7	29	14.9	16
8	**4**	2	8.4	13	6.7	7
9	**5**	2	0	0	1.8	2
10	Mo(0) powder	2	0	0	0	0
11	MoO_3 powder	2	0	0	0	0

[a]Data are the mean of multiple individual experiments (at least two) with error bars representing standard deviation. [b]Data are the same as Table 1, entry 10.

Gaseous NH_3 generation by mechanochemical nitrogen fixation

Importantly, the mechanochemical nitrogen fixation we developed here enables the collection of gaseous NH_3 directly from reaction vessel without using any solvents. At the beginning of the project, we expected that gaseous NH_3 can be obtained directly from the milling jar after the reaction thanks to the nature of the gas–solid reaction, which does not involve any solvent to dissolve NH_3. However, contrary to our initial expectation, gaseous NH_3 in the milling jar (defined as gas-phase NH_3; Methods) was not observed in all the entries in Tables 1 and 2, probably due to the Lewis acid–base pair formation between Sm(III) species and NH_3. In these cases, NH_3 trapped in the solid mixture (defined as solid-phase NH_3; Methods) was quantified by (1) transferring the solid mixtures to the flask with THF, (2) adding aqueous potassium hydroxide (KOH) solution to the mixture and then (3) distilling volatiles and trapping them into a dilute H_2SO_4 solution. To generate gas-phase NH_3 without using any solvents during the whole process, we have developed a two-step procedure to selectively generate gas-phase NH_3 over solid-phase NH_3 using solid KOH as the Brønsted base (Supplementary Fig. 7). First, the mechanochemical reaction was carried out in the same manner as Table 2, entry 5 using 3,600 equiv. (0.36 mmol) of $SmI_2(THF)_2$ and 3,600 equiv. (0.36 mmol) of pentaerythritol in the presence of a catalytic amount of complex **1b** (0.1 μmol) under N_2 atmosphere. Then, solid KOH (2.7 mmol) was added to the milling jar and the mixture was subjected to ball milling for a further 1 h. After this two-step process, 520 equiv. of gas-phase NH_3 based on the catalyst were generated selectively without the use of solvents. We unambiguously identified the gas-phase NH_3 thus formed by Fourier-transform infrared measurement (Supplementary Fig. 15) as well as by colourimetric analysis.

Investigation of reaction mechanism

To elucidate the reaction pathway of mechanochemical nitrogen fixation, we first investigated how the activation of the nitrogen–nitrogen triple bond of N_2 occurs at molybdenum complex **1a** under mechanochemical conditions. The mechanochemical reaction of molybdenum triiodide complex **1a** with 5 equiv. of $SmI_2(THF)_2$ was conducted under N_2 atmosphere. After reaction for 10 min, the reaction mixture was dissolved in THF-d_8 under Ar atmosphere to measure ^1H and $^{31}P\{^1H\}$ NMR spectroscopy, and it was revealed that a molybdenum–nitride complex (**2**) was formed in 34% NMR yield (Fig. 3a and Supplementary Figs. 8 and 9). The electrospray ionization time-of-flight mass spectrometry spectrum of the reaction mixture in THF also supported the formation of complex **2** (Supplementary Fig. 10). These results suggested that nitride complex **2** was formed via direct cleavage of the nitrogen–nitrogen triple bond under mechanochemical conditions (Fig. 3c, green). To gain further insight into the solid reaction mixture, we conducted Mo K-edge X-ray absorption measurements. The X-ray absorption near-edge structure spectrum of the solid reaction mixture showed a pre-edge peak indicative of complex **2** (Supplementary Fig. 11a)[47]. The observed spectrum of the solid reaction mixture was reproduced well by linear combination fitting of the spectra of nitride complex **2** (67%) and unreacted **1a** (33%) (Supplementary Fig. 11b). We also analysed the extended X-ray absorption fine structure spectrum of the reaction mixture. The Fourier-transformed extended X-ray absorption fine structure spectra (Supplementary Fig. 12) of the reaction mixture showed a decrease in the band intensity of molybdenum–iodine scattering at around 2.6 Å compared with complex **1a**, suggesting that the iodide ligand in complex **1a** was removed from the molybdenum centre by the reaction with N_2 and $SmI_2(THF)_2$. These results all support that the direct cleavage of the nitrogen–nitrogen triple bond took place between the molybdenum complexes and N_2 at the gas–solid interface (Fig. 3c).

We next investigated the nitrogen–hydrogen bond formation process (Fig. 3c, orange). When complex **2** was allowed to react with 5 equiv. of $SmI_2(THF)_2$ and 5 equiv. of pentaerythritol under mechanochemical conditions for 1 h, quantitative formation of NH_3 was observed (Fig. 3b). Furthermore, complex **2** showed catalytic activity comparable to **1a** under mechanochemical conditions (Table 2, entry 6). These experimental results indicate that molybdenum–nitride complex **2** served as a reactive intermediate under mechanochemical conditions through the subsequent formation of nitrogen–hydrogen bonds.

The nitrogen–hydrogen bond formation under mechanochemical conditions shown above is consistent with that under homogeneous conditions using $SmI_2(THF)_2$ and H_2O, where the nitride complex **2** was protonated and reduced in a concerted manner (PCET) by the $SmI_2(H_2O)$ complex[45] to give imide, amide and ammine complexes[37]. In relation to this, we examined whether the combination of $SmI_2(THF)_2$ and pentaerythritol can be applicable to other PCET reactions under mechanochemical conditions. Reduction of aromatic hydrocarbons is known as a typical PCET reaction under homogeneous conditions[48,49]. Therefore, we carried out reactions of anthracene or *trans*-stilbene with 3 equiv. of $SmI_2(THF)_2$ and 6 equiv. of pentaerythritol under mechanochemical conditions. As a result, 9,10-dihydroanthracene and 1,2-diphenylethane were obtained in 87% and 37% NMR yield, respectively (Figs. 4a,b). The progress of these two reactions indicates that the bond-dissociation free energy (BDFE) values of the carbon–hydrogen bonds in the reaction intermediates (Fig. 4c, 36.3 and 34.1 kcal mol^{-1}

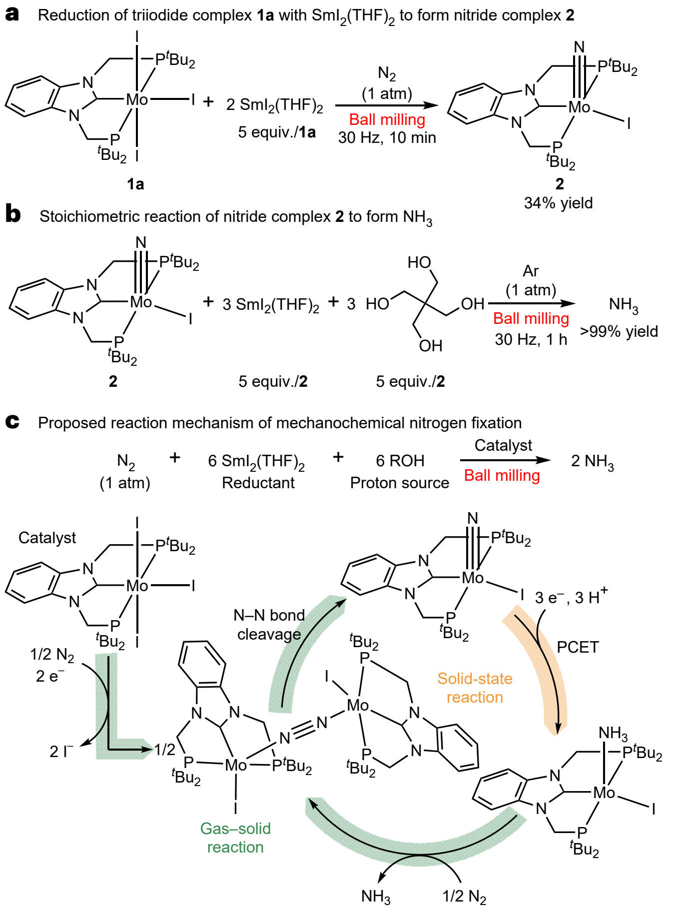
a Reduction of triiodide complex **1a** with $SmI_2(THF)_2$ to form nitride complex **2**

b Stoichiometric reaction of nitride complex **2** to form NH_3

c Proposed reaction mechanism of mechanochemical nitrogen fixation

Fig. 3 | Stoichiometric reactions and proposed reaction mechanism for mechanochemical nitrogen fixation. a, The reduction of molybdenum triiodide complex **1a** with $SmI_2(THF)_2$ to afford nitride complex **2** under mechanochemical conditions. **b**, The stoichiometric reaction to generate NH_3 from nitride complex **2** under mechanochemical conditions. **c**, A plausible reaction pathway of mechanochemical nitrogen fixation that involves nitrogen–nitrogen bond cleavage (gas–solid reaction) and nitrogen–hydrogen bond formation by PCET (solid-state reaction).

for anthracene and *trans*-stilbene, respectively[49]) are greater than that of the oxygen–hydrogen bond of pentaerythritol combined with $SmI_2(THF)_2$. In addition, it is reasonable that the nitrogen–hydrogen bond formation on nitride complex **2** proceeds smoothly by the PCET process, considering the BDFE value of the nitrogen–hydrogen bond of the imide complex (Fig. 4c, 33.8 kcal mol^{-1}(ref. 37)) is similar to those of the carbon–hydrogen bonds discussed above. Currently, we do not know why the reaction of *trans*-stilbene (Fig. 4b) is relatively slow compared with the nitrogen–hydrogen bond formation on nitride complex **2** (Fig. 3b) with almost the same BDFE values; however, this may be due to the difference between BDFE values in solution state and in the solid state or due to other factors unique to mechanochemical reactions. Further, isotope labelling experiments for anthracene reduction using deuterated pentaerythritol were carried out, and the kinetic isotope effect (KIE) value was determined to be 1.3 (Fig. 4d), thereby proving anthracene reduction by $SmI_2(THF)_2$ and pentaerythritol to be the PCET reaction. These results clearly demonstrate that the combination of $SmI_2(THF)_2$ and pentaerythritol can be used to form nitrogen–hydrogen or carbon–hydrogen bonds employing the PCET process in the solid phase.

Based on these stoichiometric reactions, we hypothesized the reaction pathway as follows (Fig. 3c). The molybdenum triiodide complex **1a** was reduced to give nitride complex **2** via direct cleavage of the nitrogen–nitrogen triple bond at the gas–solid interface. Then, the nitride complex **2** reacted with $SmI_2(THF)_2$ and proton sources via the PCET process to give the corresponding ammine complex in the solid phase. The ammine complex was further converted into the nitride complex **2** again by ligand exchange from NH_3 to N_2 and direct nitrogen–nitrogen bond cleavage to complete the catalytic cycle.

From a practical viewpoint, two big drawbacks in the homogeneous catalytic nitrogen fixation using SmI_2 and H_2O in the presence of molybdenum catalysts are the high cost of solvent (THF) even if the solvent is recycled, and the extra energy and cost needed to separate gaseous NH_3 from the THF and water mixture. Therefore, our mechanochemical nitrogen fixation has clear advantages to avoid the use of the solvent to reduce process cost, complexity of the process, and the extra energy compared with the corresponding solution-state reaction. In fact, after the corresponding homogeneous reaction in THF, we need to liberate gas-phase NH_3 from a mixed solution of THF and water. This is energetically quite demanding because it involves the dehydration of NH_3, vapourization of THF and vapourization of water, all known as highly endothermic processes with $\Delta H = 8.1$, 7.6 and 10.5 kcal mol^{-1}, respectively. These physical processes require energy comparable to the chemical processes of interest (for example, chemical overpotential of the current system using SmI_2 and water is estimated to be ~44 kcal mol^{-1} (refs. 36,49)). Therefore, we cannot ignore the energy required for these processes, and consideration of these issues is essential from the viewpoint of practical application in the near future. In addition, we estimated the cost of THF required to produce 1 mol of NH_3. In a typical procedure in our homogeneous reaction[37], THF solvent (about 50 l) is required for the reaction, which costs as much as 4,000 USD. Such substantial differences between

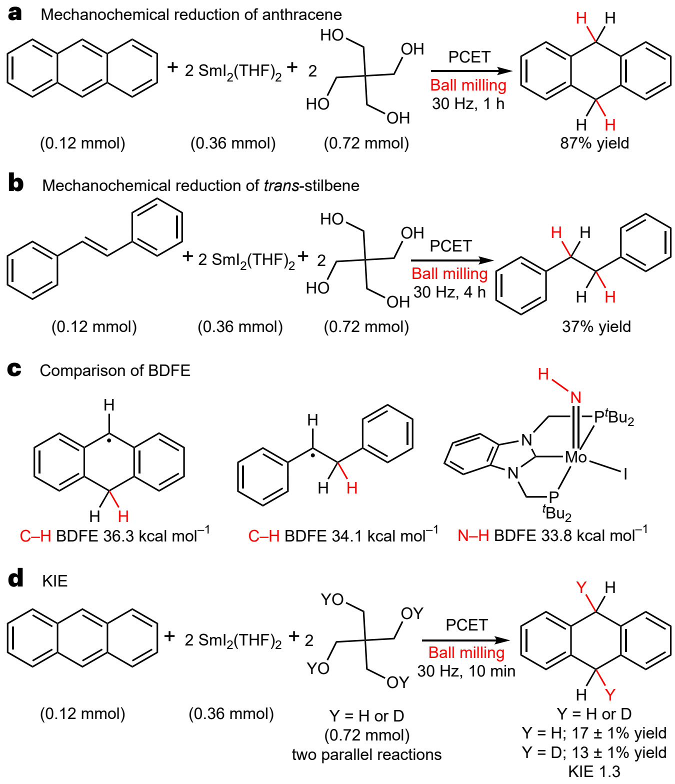
a Mechanochemical reduction of anthracene

b Mechanochemical reduction of *trans*-stilbene

c Comparison of BDFE

d KIE

Fig. 4 | Investigation on PCET processes under mechanochemical conditions. a, The mechanochemical reduction of anthracene with $SmI_2(THF)_2$ and pentaerythritol. **b**, The mechanochemical reduction of *trans*-stilbene with $SmI_2(THF)_2$ and pentaerythritol. **c**, A comparison of BDFE to form carbon–hydrogen or nitrogen–hydrogen bonds. **d**, Isotope labelling experiments to evaluate the KIE in the reduction of anthracene under mechanochemical conditions.

homogeneous and mechanochemical systems will be critical to achieve mass production of NH_3.

Conclusion

We have developed catalytic mechanochemical nitrogen fixation using molecular catalysts under solvent-free ball-milling conditions. We investigated the various proton sources to find that water, alcohols and even sugars can be applicable to the nitrogen fixation under mechanochemical conditions. Mechanochemical nitrogen fixation we developed not only allows the use of some proton sources that were difficult to use in homogeneous conditions but also the selective generation of gaseous NH_3. We also carried out stoichiometric reactions under mechanochemical conditions to gain insight into the mechanochemical reaction catalysed by transition metal complexes involving gaseous reactants. We believe that the results presented in this study contribute to the further development of novel mechanochemical gas–solid reactions under mild and eco-friendly conditions.

Methods

Typical procedures for mechanochemical nitrogen fixation

In an Ar-filled glovebox, $SmI_2(THF)_2$ (198 mg, 0.36 mmol), pentaerythritol (49.0 mg, 0.36 mmol), $MoI_3(PCP)$ (1.9 mg, 0.002 mmol) and a stainless-steel ball (diameter: 10.0 mm) were added in a stainless-steel milling jar (~5 ml). The jar was filled with N_2 (~1 atm) in a N_2-filled glovebox. The jar was tightly capped and placed in a grinding vessel (Retsch MM400; Supplementary Fig. 1). After grinding by ball mill at 30 Hz for 1 h, the jar was opened in a sealed bag (GL Science Smart Bag PA, cat. no. 3008-97701; Supplementary Fig. 2) containing air. An aliquot (typically 100 µl) of gas inside the bag was sampled and subjected to gas chromatography measurements to quantify the amount of generated dihydrogen (H_2). Then, the gas inside the bag was blown into a dilute H_2SO_4 solution (0.5 M, 10 ml) to trap gaseous NH_3 (defined as gas-phase NH_3). At that point, the reaction mixture looked yellow when $SmI_2(THF)_2$ was totally consumed by the reaction (Supplementary Fig. 3b). If unreacted $SmI_2(THF)_2$ remained after the reaction, the reaction mixture showed a black or dark-blue colour just after opening the jar (Supplementary Fig. 3c), and the mixture was gradually quenched by the air to give a yellow-coloured solid (Supplementary Fig. 3d). After confirming that the reaction mixture was quenched entirely, the solid reaction mixture was transferred to a 50 ml Schlenk flask with water or THF (~6 ml). Aqueous potassium hydroxide (KOH) solution (30 wt%, 5 ml) was added to the suspension containing the reaction mixture in the Schlenk flask, and volatiles were trapped by dilute H_2SO_4 solution (0.5 M, 10 ml). Trapped NH_3 in the solid reaction mixture was defined as solid-phase NH_3. The amount of NH_3 present in each H_2SO_4 solution (corresponding to gas-phase NH_3 and solid-phase NH_3, respectively) was determined by the indophenol method[50]. The procedure for the indophenol method is as follows. A suitably diluted H_2SO_4 solution that contains trapped $NH_3$was added to an aqueous solution of PhOH and $Na_2[Fe(CN)_5(NO)]$, and the mixture was shaken vigorously. Then, an aqueous solution of NaOH and NaClO was added, mixed thoroughly and stood at room temperature for 3 h to afford a blue solution. The amount of NH_3 was determined on the basis of the absorbance at 634 nm. Unless otherwise noted, the yield of NH_3 was defined as the sum of the gas-phase NH_3 and the solid-phase NH_3. No hydrazine was detected by the *p*-(dimethylamino)benzaldehyde method[51]. The procedure for the *p*-(dimethylamino)benzaldehyde method is as follows. A suitably diluted H_2SO_4 solution that potentially contains trapped hydrazine was added to a solution of *p*-(dimethylamino)benzaldehyde and HCl in EtOH, and the mixture was shaken vigorously. Then, a diluted HCl solution was added, mixed thoroughly and stood at room temperature for 3 h. The amount of NH_3 was determined on the basis of the absorbance at 458 nm.

Data availability

The data that support the findings of this study are available in this Article and its Supplementary Information. Crystallographic data for the structure reported in this article have been deposited at the Cambridge Crystallographic Data Centre, under deposition number CCDC 2369997 (dinuclear Sm(III)–pentaerythritol complex). Copies of the data can be obtained free of charge via https://www.ccdc.cam.ac.uk/structures/. Source data are provided with this paper.

References

1. James, S. L. et al. Mechanochemistry: opportunities for new and cleaner synthesis. *Chem. Soc. Rev.* **41**, 413–447 (2012).
2. Kubota, K. & Ito, H. Mechanochemical cross-coupling reactions. *Trends Chem* **2**, 1066–1081 (2020).
3. Do, J.-L. & Friščić, T. Mechanochemistry: a force of synthesis. *ACS Cent. Sci.* **3**, 13–19 (2017).
4. Howard, J. L., Cao, Q. & Browne, D. L. Mechanochemistry as an emerging tool for molecular synthesis: what can it offer? *Chem. Sci.* **9**, 3080–3094 (2018).
5. Porcheddu, A., Colacino, E., De Luca, L. & Delogu, F. Metal-mediated and metal-catalyzed reactions under mechanochemical conditions. *ACS Catal.* **10**, 8344–8394 (2020).
6. Jiang, Z.-J., Li, Z.-H., Yu, J.-B. & Su, W.-K. Liquid-assisted grinding accelerating: Suzuki–Miyaura reaction of aryl chlorides under high-speed ball-milling conditions. *J. Org. Chem.* **81**, 10049–10055 (2016).
7. Seo, T., Ishiyama, T., Kubota, K. & Ito, H. Solid-state Suzuki–Miyaura cross-coupling reactions: olefin-accelerated C–C coupling using mechanochemistry. *Chem. Sci.* **10**, 8202–8210 (2019).
8. Vogt, C. G. et al. Direct mechanocatalysis: palladium as milling media and catalyst in the mechanochemical Suzuki polymerization. *Angew. Chem. Int. Ed.* **58**, 18942–18947 (2019).
9. Seo, T., Kubota, K. & Ito, H. Selective mechanochemical monoarylation of unbiased dibromoarenes by in situ crystallization. *J. Am. Chem. Soc.* **142**, 9884–9889 (2020).
10. Seo, T., Toyoshima, N., Kubota, K. & Ito, H. Tackling solubility issues in organic synthesis: solid-state cross-coupling of insoluble aryl halides. *J. Am. Chem. Soc.* **143**, 6165–6175 (2021).
11. Gao, Y., Feng, C., Seo, T., Kubota, K. & Ito, H. Efficient access to materials-oriented aromatic alkynes *via* the mechanochemical Sonogashira coupling of solid aryl halides with large polycyclic conjugated systems. *Chem. Sci.* **13**, 430–438 (2022).
12. Kubota, K., Seo, T., Koide, K., Hasegawa, Y. & Ito, H. Olefin-accelerated solid-state C–N cross-coupling reactions using mechanochemistry. *Nat. Commun.* **10**, 111 (2019).
13. Shao, Q.-L., Jiang, Z.-J. & Su, W.-K. Solvent-free mechanochemical Buchwald–Hartwig amination of aryl chlorides without inert gas protection. *Tetrahedron Lett.* **59**, 2277–2280 (2018).
14. Cao, Q., Howard, J. L., Wheatley, E. & Browne, D. L. Mechanochemical activation of zinc and application to Negishi cross-coupling. *Angew. Chem. Int. Ed.* **57**, 11339–11343 (2018).
15. Pang, Y., Ishiyama, T., Kubota, K. & Ito, H. Iridium(I)-catalyzed C–H borylation in air by using mechanochemistry. *Chem. Eur. J.* **25**, 4654–4659 (2019).
16. Do, J.-L., Mottillo, C., Tan, D., Štrukil, V. & Friščić, T. Mechanochemical ruthenium-catalyzed olefin metathesis. *J. Am. Chem. Soc.* **137**, 2476–2479 (2015).
17. Lee, G. S. et al. Mechanochemical ring-opening metathesis polymerization: development, scope, and mechano-exclusive polymer synthesis. *Chem. Sci.* **13**, 11496–11505 (2022).
18. Hermann, G. N. & Bolm, C. Mechanochemical rhodium(III)-catalyzed C–H bond amidation of arenes with dioxazolones under solventless conditions in a ball mill. *ACS Catal.* **7**, 4592–4596 (2017).

19. Cheng, H., Hernández, J. G. & Bolm, C. Mechanochemical cobalt-catalyzed C–H bond functionalizations by ball milling. *Adv. Synth. Catal.* **360**, 1800–1804 (2018).
20. Cousin, K., Menuel, S., Monflier, E. & Hapiot, F. Hydroformylation of alkenes in a planetary ball mill: from additive-controlled reactivity to supramolecular control of regioselectivity. *Angew. Chem. Int. Ed.* **56**, 10564–10568 (2017).
21. Hermann, G. N., Becker, P. & Bolm, C. Mechanochemical rhodium(III)-catalyzed C–H bond functionalization of acetanilides under solventless conditions in a ball mill. *Angew. Chem. Int. Ed.* **54**, 7414–7417 (2015).
22. Bolm, C. & Hernández, J. G. Mechanochemistry of gaseous reactants. *Angew. Chem. Int. Ed.* **58**, 3285–3299 (2019).
23. Smidt, J. et al. Katalytische Umsetzungen von Olefinen an Platinmetall-Verbindungen Das Consortium-Verfahren zur Herstellung von Acetaldehyd. *Angew. Chem.* **71**, 176–182 (1959).
24. Wilke, G. Fifty years of Ziegler catalysts: consequences and development of an invention. *Angew. Chem. Int. Ed.* **42**, 5000–5008 (2003).
25. Sinn, H., Kaminsky, W., Vollmer, H. & Woldt, R. "Living polymers" on polymerization with extremely productive Ziegler catalysts. *Angew. Chem. Int. Ed. Engl.* **19**, 390–392 (1980).
26. Noyori, R. Asymmetric catalysis: science and opportunities (Nobel Lecture 2001). *Adv. Synth. Catal.* **345**, 15–32 (2003).
27. Foster, S. L. et al. Catalysts for nitrogen reduction to ammonia. *Nat. Catal.* **1**, 490–500 (2018).
28. Boerner, L. K. Taking the CO_2 out of NH_3. *C&EN Global Enterprise* **97**, 18–21 (2019).
29. MacFarlane, D. R. et al. A roadmap to the ammonia economy. *Joule* **4**, 1186–1205 (2020).
30. Han, G.-F. et al. Mechanochemistry for ammonia synthesis under mild conditions. *Nat. Nanotechnol.* **16**, 325–330 (2021).
31. Reichle, S., Felderhoff, M. & Schüth, F. Mechanocatalytic room-temperature synthesis of ammonia from its elements down to atmospheric pressure. *Angew. Chem. Int. Ed.* **60**, 26385–26389 (2021).
32. Tricker, A. W. et al. Mechanocatalytic ammonia synthesis over TiN in transient microenvironments. *ACS Energy Lett.* **5**, 3362–3367 (2020).
33. Arashiba, K., Miyake, Y. & Nishibayashi, Y. A molybdenum complex bearing PNP-type pincer ligands leads to the catalytic reduction of dinitrogen into ammonia. *Nat. Chem.* **3**, 120–125 (2011).
34. Eizawa, A. et al. Remarkable catalytic activity of dinitrogen-bridged dimolybdenum complexes bearing NHC-based PCP-pincer ligands toward nitrogen fixation. *Nat. Commun.* **8**, 14874 (2017).
35. Arashiba, K. et al. Catalytic nitrogen fixation via direct cleavage of nitrogen–nitrogen triple bond of molecular dinitrogen under ambient reaction conditions. *Bull. Chem. Soc. Jpn* **90**, 1111–1118 (2017).
36. Ashida, Y., Arashiba, K., Nakajima, K. & Nishibayashi, Y. Molybdenum-catalysed ammonia production with samarium diiodide and alcohols or water. *Nature* **568**, 536–540 (2019).
37. Ashida, Y. et al. Catalytic production of ammonia from dinitrogen employing molybdenum complexes bearing N-heterocyclic carbene-based PCP-type pincer ligands. *Nat. Synth.* **2**, 635–644 (2023).
38. Yandulov, D. V. & Schrock, R. R. Catalytic reduction of dinitrogen to ammonia at a single molybdenum center. *Science* **301**, 76–78 (2003).
39. Masero, F., Perrin, M. A., Dey, S. & Mougel, V. Dinitrogen fixation: rationalizing strategies utilizing molecular complexes. *Chem. Eur. J.* **27**, 3892–3928 (2021).
40. Tanabe, Y. & Nishibayashi, Y. Comprehensive insights into synthetic nitrogen fixation assisted by molecular catalysts under ambient or mild conditions. *Chem. Soc. Rev.* **50**, 5201–5242 (2021).
41. Chalkley, M. J., Drover, M. W. & Peters, J. C. Catalytic N_2-to-NH_3 (or -N_2H_4) conversion by well-defined molecular coordination complexes. *Chem. Rev.* **120**, 5582–5636 (2020).
42. Tanabe, Y. & Nishibayashi, Y. Catalytic nitrogen fixation using well-defined molecular catalysts under ambient or mild reaction conditions. *Angew. Chem. Int. Ed.* https://doi.org/10.1002/anie.202406404 (2024).
43. Friščić, T., Childs, S. L., Rizvic, S. A. A. & Jones, W. The role of solvent in mechanochemical and sonochemical cocrystal formation: a solubility-based approach for predicting cocrystallisation outcome. *CrystEngComm* **11**, 418–426 (2009).
44. Klemm, D., Heublein, B., Fink, H. & Bohn, A. Cellulose: fascinating biopolymer and sustainable raw material. *Angew. Chem. Int. Ed.* **44**, 3358–3393 (2005).
45. Yamamoto, A. et al. Coordination structure of samarium diiodide in a tetrahydrofuran–water mixture. *Inorg. Chem.* **62**, 5348–5356 (2023).
46. Ashida, Y. et al. Molybdenum-catalyzed ammonia formation using simple monodentate and bidentate phosphines as auxiliary ligands. *Inorg. Chem.* **58**, 8927–8932 (2019).
47. Yamamoto, A. et al. Structural characterization of molybdenum–dinitrogen complex as key species toward ammonia formation by dispersive XAFS spectroscopy. *Phys. Chem. Chem. Phys.* **22**, 12368–12372 (2020).
48. Chciuk, T. V. & Flowers, R. A. Proton-coupled electron transfer in the reduction of arenes by SmI_2–water complexes. *J. Am. Chem. Soc.* **137**, 11526–11531 (2015).
49. Bartulovich, C. O. & Flowers, R. A. Coordination-induced O–H bond weakening in Sm(II)–water complexes. *Dalton Trans.* **48**, 16142–16147 (2019).
50. Weatherburn, M. W. Phenol–hypochlorite reaction for determination of ammonia. *Anal. Chem.* **39**, 971–974 (1967).
51. Watt, G. W. & Chrisp, J. D. A spectrophotometric method for the determination of hydrazine. *Anal. Chem.* **24**, 2006–2008 (1952).

Acknowledgements

We thank Grants-in-Aids for Scientific Research (nos. JP20H05671, 22K19041, 24H00049, 24H01834 and 24K21778 to Y.N. and 23K13758 to S.S.) from JSPS. This paper is based on results obtained from a project, JPNP21020, commissioned by the New Energy and Industrial Technology Development Organization (NEDO). The Mo K-edge X-ray absorption measurements were performed at the NW10A beamline of the Photon Factory (proposal no. 2022G549).

Author contributions

Y.N. conceived and designed this project. S.S., K.M. and A.Y. conducted the experimental works. S.S., K.M., A.Y. and H.Y. analysed the X-ray absorption data. All authors discussed the results and drafted the manuscript.

Competing interests

The authors declare no competing interests.

Additional information

Supplementary information The online version contains supplementary material available at https://doi.org/10.1038/s44160-024-00661-y.

Correspondence and requests for materials should be addressed to Yoshiaki Nishibayashi.

Peer review information *Nature Synthesis* thanks the anonymous reviewers for their contribution to the peer review of this work. Primary handling editor: Peter Seavill, in collaboration with the *Nature Synthesis* team.

Reprints and permissions information is available at www.nature.com/reprints.

Publisher's note Springer Nature remains neutral with regard to jurisdictional claims in published maps and institutional affiliations.

Open Access This article is licensed under a Creative Commons Attribution-NonCommercial-NoDerivatives 4.0 International License, which permits any non-commercial use, sharing, distribution and reproduction in any medium or format, as long as you give appropriate credit to the original author(s) and the source, provide a link to the Creative Commons licence, and indicate if you modified the licensed material. You do not have permission under this licence to share adapted material derived from this article or parts of it. The images or other third party material in this article are included in the article's Creative Commons licence, unless indicated otherwise in a credit line to the material. If material is not included in the article's Creative Commons licence and your intended use is not permitted by statutory regulation or exceeds the permitted use, you will need to obtain permission directly from the copyright holder. To view a copy of this licence, visit http://creativecommons.org/licenses/by-nc-nd/4.0/.

© The Author(s) 2024